Vol 13 No 9, September 2004
1009-1963/2004/13(09)/1500-10

Chinese Physics

© 2004 Chin. Phys. Soc.
and IOP Publishing Ltd

Evolution of local ideal helical perturbations in cylindrical plasma*

Zhang Wen-Lu(张文禄) and Li Ding(李 定)†

Department of Modern Physics, University of Science and Technology of China, Hefei 230027, China

(Received 15 March 2004)

The evolution of a local helical perturbation and its stability property for arbitrary magnetic shear configurations are investigated for the case of in cylindrical geometry. An analytic stability criterion has been obtained which predicts that a strong magnetic shear will enhance the instability in the positive shear region but enhance the stability in the negative shear region. The perturbations with the poloidal and toroidal perturbation mode numbers $m/n = 1/1$ is most unstable due to the stabilizing terms increasing with m. For $m/n = 1/1$ local perturbations in the conventional positive magnetic shear (PMS) configurations, a larger $q_{\min}$ exhibits a weaker shear in the core and is favourable to the stability, while in the reversed magnetic shear (RMS) configurations, a larger q_0 corresponds to a stronger positive shear in the middle region, which enhances the instability. No instabilities are found for $m \geq 2$ local perturbations. The stability for RMS configuration is not better than that for PMS configuration.

Keywords: time expanding method, local ideal helical perturbation, cylindrical plasma
PACC: 5235P, 5255

1. Introduction

Different from the conventional positive magnetic shear (PMS) configuration whose safety factor q is monotonic, the reversed magnetic shear (RMS) configuration with a non-monotonic safety factor q leads to the promising candidates for high bootstrap fraction and steady state Tokamak operation, which is an ultimate objective for the next generation controlled fusion devices, for example the International Thermonuclear Experimental Research (ITER). However, to what extent the adequately stable profiles can be realized in reactors remains an open problem. Investigation of the ideal and resistive magnetohydrodynamic (MHD) instabilities for RMS scenarios becomes an essential issue to understand the improvement of plasma confinement behaviour.

Much of the basic insight and the more complete understanding concerning the MHD instabilities is due to Shafranov,[1] Wesson,[2] Beteman,[3] Freidberg[4] and Mirnov *et al.*[5] Advantageous aspects of the RMS via simulation were reported by Kessel *et al*[6] for the improvements in the maximum stable thermal pressure, the bootstrap current contribution, and kinetic stability to temperature and density gradient driven modes in toroidal geometry. This was first inspected by Levinton *et al*[7] on the Tokamak Fusion Test Reactor (TFTR), where particle and ion thermal diffusivities decrease by a factor of at least 40 to the neoclassical level in the reversed shear region. Almost simultaneously this observation was confirmed by Strait *et al*[8] in DIII-D H-mode discharges in which ballooning modes are stabilized while beta and energy confinement are better than L-mode. Further experimental support was given by Lazarus *et al*[9] for power gain increased 3 times in DIII-D. In 1996, Gimblett *et al*[10] obtained an analytical criterion for RMS profiles by expanding in inverse aspect ratio and assuming that the minimum safety factor q_m is a shade below m/n. The resistive instabilities in reversed shear are reported by Gunter *et al*[11] and Takeji *et al.*[12]

An analytic method was introduced by Psimopoulos and Haines[13] to describe the early time evolution of a perturbation in plasma. This method was applied by Psimopoulos and Li[14] to inquire the stabilizing effect of a longitudinal magnetic field on the evolution of a helical perturbations with $m = 1$ in a cylindrical plasma for the PMS configuration. This method im-

*Project supported by the National Natural Science Foundation of China (Grant Nos 10175065, 40244006, 40336052).
†E-mail: dli@ustc.edu.cn

poses no extra assumptions to instability because the criterion can be naturally derived by comparing the second order acceleration with the initial perturbation, which makes the criterion not only sufficient but also necessary for instability. The aim of the present work is to investigate the short time evolution of ideal local helical perturbations and its stability properties with poloidal perturbation mode number $m \geq 1$ in a cylindrical plasma where an arbitrary magnetic shear configuration is considered.

Generally, the evolution of an arbitrary perturbation, $\boldsymbol{V}[\boldsymbol{x}_f(\boldsymbol{x},t),t]$, can be investigated via time series:

$$\boldsymbol{V}(\boldsymbol{x},t) = \boldsymbol{V}_0(\boldsymbol{x}) + \left(\frac{\mathrm{d}\boldsymbol{V}}{\mathrm{d}t}\right)_0 t + \left(\frac{\mathrm{d}^2\boldsymbol{V}}{\mathrm{d}t^2}\right)_0 \frac{t^2}{2!} + \cdots, \quad (1)$$

where $\boldsymbol{V}_0(\boldsymbol{x})$ is an arbitrary nonzero initial perturbation and the coefficients $(\mathrm{d}^i\boldsymbol{V}/\mathrm{d}t^i)_0$, $i = 1, 2, \ldots$, can be immediately derived from the ideal MHD equations. Therefore, $\boldsymbol{V}(\boldsymbol{x},t)$ and $(\mathrm{d}^i\boldsymbol{V}/\mathrm{d}t^i)_0$ depend only on the initial position $\boldsymbol{x}$ of the fluid element.

The basic equations and assumptions used in this work are introduced in Section 2. By employing ideal MHD equations, in Section 3, the local helical perturbation velocity is expanded in time series up to the second order. In Section 4, the stability against ideal local helical perturbations is analyzed for PMS and RMS respectively, where we dwell on the $m/n = 1/1$ perturbation rather than the $m > 1$ perturbations. All the current profiles, J_{z0}, vanish at the plasma boundary. Finally, conclusions are stated in the last section.

2. Basic equations and assumptions

A steady state plasma is considered in this work. The perturbation velocity $\boldsymbol{V}$, mass density ρ, thermal pressure p, current density $\boldsymbol{J}$ and magnetic field $\boldsymbol{B}$ are described by the ideal MHD equations:

$$\frac{\mathrm{d}\boldsymbol{V}}{\mathrm{d}t} = \frac{1}{\rho}\left(-\nabla p + \boldsymbol{J}\times\boldsymbol{B}\right), \quad (2)$$

$$\frac{\partial\boldsymbol{B}}{\partial t} = \nabla\times\left(\boldsymbol{V}\times\boldsymbol{B}\right), \quad (3)$$

$$\nabla\times\boldsymbol{B} = \mu_0\,\boldsymbol{J}, \quad (4)$$

$$\frac{\mathrm{d}\rho}{\mathrm{d}t} = -\rho\,\left(\nabla\cdot\boldsymbol{V}\right), \quad (5)$$

$$\frac{\mathrm{d}p}{\mathrm{d}t} = -\gamma\,p\,\left(\nabla\cdot\boldsymbol{V}\right), \quad (6)$$

where operator $\mathrm{d}/\mathrm{d}t$ stands for the convective derivative and γ is the ratio of specific heats. At the start, $t = 0$, the plasma is characterized in cylindrical coordinates by the profiles:

$$\rho_0 = \rho_0(r), \quad \boldsymbol{B}_0 = \hat{e}_\theta\,B_{\theta0}(r) + \hat{e}_z\,B_{z0}(r),$$

$$p_0 = p_0(r), \quad \boldsymbol{J}_0 = \hat{e}_\theta\,J_{\theta0}(r) + \hat{e}_z\,J_{z0}(r),$$

where $B_{\theta0}$ is produced by the longitudinal current density J_{z0} and B_{z0} is generated by the external magnetic field. These profiles are conjuncted by the equilibrium MHD equations:

$$\frac{\mathrm{d}p_0}{\mathrm{d}r} = J_{\theta0}\,B_{z0} - J_{z0}\,B_{\theta0}, \quad (7)$$

$$\frac{1}{r}\frac{\mathrm{d}\left(r\,B_{\theta0}\right)}{\mathrm{d}r} = \mu_0\,J_{z0}, \quad (8)$$

$$-\frac{\mathrm{d}B_{z0}}{\mathrm{d}r} = \mu_0\,J_{\theta0}. \quad (9)$$

Only incompressible fluid is considered in this work. Thus, suppose that there exists an initial helical perturbation $\boldsymbol{V}_0(\boldsymbol{x})$ at $t = 0$, which represents an outward motion of each section of the cylindrical plasma column and has no component in the Z-direction:

$$\boldsymbol{V}_0 = a\,\left[\hat{e}_r\,m\cos(m\theta - kz) - \hat{e}_\theta\,\sin(m\theta - kz)\right], \quad (10)$$

where a=const. represents a local perturbation, k is the longitudinal wave number and because of the incompressibility the initial perturbation (10) has a zero divergence, namely

$$\nabla\cdot\boldsymbol{V}_0 = \frac{a}{r}\frac{\partial}{\partial r}\left[r\,m\,\cos(m\theta - kz)\right] - \frac{a}{r}\frac{\partial}{\partial\theta}\left[\sin(m\theta - kz)\right] = 0.$$

3. Derivation of the second order acceleration

The coefficients $(\mathrm{d}^i\boldsymbol{V}/\mathrm{d}t^i)_0$, $i = 1, 2, \ldots$, of time series (1) are going to be calculated up to the second order by employing the ideal MHD Equations (2)–(6). According to the momentum equation (2), the first order acceleration is zero at time $t = 0$, namely

$$\left(\frac{\mathrm{d}\boldsymbol{V}}{\mathrm{d}t}\right)_0 = \frac{1}{\rho_0}\left(-\nabla p_0 + \boldsymbol{J}_0\times\boldsymbol{B}_0\right) = 0, \quad (11)$$

which is naturally held by equilibrium equation (7). Thus it is necessary to consider the second order acceleration of the perturbation to obtain a stability criterion. In order to calculate the second order acceleration, $(\mathrm{d}^2\boldsymbol{V}/\mathrm{d}t^2)_0$, the momentum equation (2) is differentiated with regard to time:

$$\frac{\mathrm{d}^2\boldsymbol{V}}{\mathrm{d}t} = \frac{1}{\rho}\frac{\mathrm{d}}{\mathrm{d}t}\left(-\nabla p + \boldsymbol{J}\times\boldsymbol{B}\right) - \frac{1}{\rho}\frac{\mathrm{d}\rho}{\mathrm{d}t}\frac{\mathrm{d}\boldsymbol{V}}{\mathrm{d}t}. \quad (12)$$

If Equation (11) is considered, the second term in the right hand side (RHS) vanishes at $t = 0$:

$$\left(\frac{\mathrm{d}^2\boldsymbol{V}}{\mathrm{d}t^2}\right)_0 = \frac{1}{\rho_0}\left[\frac{\mathrm{d}}{\mathrm{d}t}\left(-\nabla p + \boldsymbol{J}\times\boldsymbol{B}\right)\right]_{t=0}. \quad (13)$$

The thermal pressure and the Lorentz force parts in the RHS of Eq.(13) will be calculated later one by one. It can be easily concluded by considering Eqs.(6) that the convective derivative of the thermal pressure at $t = 0$ is zero:

$$\left(\frac{\mathrm{d}p}{\mathrm{d}t}\right)_0 = -\gamma\, p_0\, (\nabla\cdot\boldsymbol{V}_0) = 0,$$

which shows that pressure stays constant along the first order displacement. The derivative of the thermal pressure can be expressed as

$$\left(\frac{\partial p}{\partial t}\right)_0 = -\left(\boldsymbol{V}_0\cdot\nabla p_0\right) = -a\,m\,\frac{\mathrm{d}p_0}{\mathrm{d}r}\,\cos(m\theta - kz).$$

Based on the above consideration the pressure part in the RHS of Eq.(13) is derived as

$$\begin{aligned}\left[\frac{\mathrm{d}}{\mathrm{d}t}\left(-\nabla p\right)\right]_{t=0} =& -\nabla\left(\frac{\partial p}{\partial t}\right)_0 - \left(\boldsymbol{V}_0\cdot\nabla\right)\nabla p_0\\ =& -\hat{e}_\theta\, a\,\frac{m^2-1}{r}\,\frac{\mathrm{d}p_0}{\mathrm{d}r}\,\sin(m\theta-kz)\\ &+\hat{e}_z\, a\,m\,k\,\frac{\mathrm{d}p_0}{\mathrm{d}r}\,\sin(m\theta-kz). \quad (14)\end{aligned}$$

The Lorentz force part is studied next. The local derivative of the magnetic field at $t = 0$ is calculated by substituting the expressions of the perturbation velocity $\boldsymbol{V}_0$ and the magnetic field $\boldsymbol{B}_0$ into Eq.(3),

$$\begin{aligned}\left(\frac{\partial\boldsymbol{B}}{\partial t}\right)_0 =& \nabla\times\left(\boldsymbol{V}_0\times\boldsymbol{B}_0\right)\\ =& -\hat{e}_r\, a\,m\,\left(\frac{m}{r}\,B_{\theta 0} - k\,B_{z0}\right)\,\sin(m\theta-kz)\\ &+\hat{e}_\theta\, a\,\left(k\,B_{z0} - m\,\frac{\mathrm{d}B_{\theta 0}}{\mathrm{d}r}\right)\,\cos(m\theta-kz)\\ &-\hat{e}_z\, a\,m\,\frac{\mathrm{d}B_{z0}}{\mathrm{d}r}\,\cos(m\theta-kz). \quad (15)\end{aligned}$$

Hence the convective derivative of the magnetic field is

$$\begin{aligned}\left(\frac{\mathrm{d}\boldsymbol{B}}{\mathrm{d}t}\right)_0 =& \left(\frac{\partial\boldsymbol{B}}{\partial t}\right)_0 + \left(\boldsymbol{V}_0\cdot\nabla\right)\,\boldsymbol{B}_0\\ =& -\hat{e}_r\, a\,\left(\frac{m^2-1}{r}\,B_{\theta 0} - m\,k\,B_{z0}\right)\\ &\times\sin(m\theta-kz)\\ &+\hat{e}_\theta\, a\,k\,B_{z0}\,\cos(m\theta-kz). \quad (16)\end{aligned}$$

Allowing for Eq.(15) and Ampere's law (4), the derivative of the current density at time $t = 0$ can be obtained as

$$\begin{aligned}\left(\frac{\partial\boldsymbol{J}}{\partial t}\right)_0 =& \frac{1}{\mu_0}\left[\nabla\times\left(\frac{\partial\boldsymbol{B}}{\partial t}\right)_0\right]\\ =& \hat{e}_r\,\frac{a}{\mu_0}\,\left(\frac{m^2}{r}\,\frac{\mathrm{d}B_{z0}}{\mathrm{d}r} + m\,k\,\frac{\mathrm{d}B_{\theta 0}}{\mathrm{d}r} - k^2\,B_{z0}\right)\,\sin(m\theta-kz)\\ &+\hat{e}_\theta\,\frac{a}{\mu_0}\,\left(-m\,k^2\,B_{z0} + \frac{m^2\,k}{r}\,B_{\theta 0} + m\,\frac{\mathrm{d}^2B_{z0}}{\mathrm{d}r^2}\right)\,\cos(m\theta-kz)\\ &+\hat{e}_z\,\frac{a}{\mu_0}\,\left[k\,\frac{\mathrm{d}B_{z0}}{\mathrm{d}r} - \frac{m}{r}\,\frac{\mathrm{d}B_{\theta 0}}{\mathrm{d}r} + \frac{m^3}{r^2}\,B_{\theta 0} - m\,\frac{\mathrm{d}^2B_{\theta 0}}{\mathrm{d}r^2} - \frac{m^2-1}{r}\,k\,B_{z0}\right]\,\cos(m\theta-kz),\end{aligned}$$

and the convective derivative of current density $\boldsymbol{J}$ at time $t = 0$ is given as

$$\begin{aligned}\left(\frac{\mathrm{d}\boldsymbol{J}}{\mathrm{d}t}\right)_0 =& \left(\frac{\partial\boldsymbol{J}}{\partial t}\right)_0 + \left(\boldsymbol{V}_0\cdot\nabla\right)\,\boldsymbol{J}_0\\ =& \hat{e}_r\,\frac{a}{\mu_0}\,\left(\frac{m^2-1}{r}\,\frac{\mathrm{d}B_{z0}}{\mathrm{d}r} + m\,k\,\frac{\mathrm{d}B_{\theta 0}}{\mathrm{d}r} - k^2\,B_{z0}\right)\,\sin(m\theta-kz)\\ &+\hat{e}_\theta\,\frac{a}{\mu_0}\,\left(-m\,k^2\,B_{z0} + \frac{m^2\,k}{r}\,B_{\theta 0}\right)\,\cos(m\theta-kz)\\ &+\hat{e}_z\,\frac{a}{\mu_0}\,\left[k\,\frac{\mathrm{d}B_{z0}}{\mathrm{d}r} + \frac{m\,(m^2-1)}{r^2}\,B_{\theta 0} - \frac{m^2-1}{r}\,k\,B_{z0}\right]\,\cos(m\theta-kz). \quad (17)\end{aligned}$$

Thus the Lorentz part of Eq.(13) can be derived as

$$\begin{aligned}\left[\frac{\mathrm{d}}{\mathrm{d}\,t}\,(\boldsymbol{J}\times\boldsymbol{B})\right]_{t=0} =& \boldsymbol{J}_0\times\left(\frac{\mathrm{d}\boldsymbol{B}}{\mathrm{d}t}\right)_0+\left(\frac{\mathrm{d}\boldsymbol{J}}{\mathrm{d}t}\right)_0\times\boldsymbol{B}_0\\ =&-\hat{e}_r\,\frac{a}{\mu_0}\left[m\,k^2\,B_{z0}^2+k\,\frac{\mathrm{d}}{\mathrm{d}r}\,(B_{\theta0}\,B_{z0})+\frac{m(m^2-1)}{r^2}\,B_{\theta0}^2\right.\\ &\left.-2\,\frac{m^2-1}{r}\,k\,B_{\theta0}\,B_{z0}\right]\cos(m\theta-kz)\\ &+\hat{e}_\theta\,\frac{a}{\mu_0}\left[k^2\,B_{z0}^2+m\,k\,\frac{B_{\theta0}\,B_{z0}}{r}-\frac{m^2-1}{r^2}\,B_{\theta0}^2-\frac{m^2-1}{2\,r}\,\frac{\mathrm{d}B_0^2}{\mathrm{d}r}\right]\sin(m\theta-kz)\\ &-\hat{e}_z\,\frac{a}{\mu_0}\left[k^2\,B_{\theta0}\,B_{z0}-\frac{m\,k}{2}\,\frac{\mathrm{d}B_0^2}{\mathrm{d}r}\right]\sin(m\theta-kz).\end{aligned}\tag{18}$$

Finally, substituting the thermal pressure part (14) and the Lorentz force part (18) into Eq.(13) and applying the equilibrium Eqs.(7)–(9), the second order acceleration of the perturbation is obtained as follows:

$$\begin{aligned}\left(\frac{\mathrm{d}^2\boldsymbol{V}}{\mathrm{d}t^2}\right)_0 =&-\hat{e}_r\,\frac{a}{\mu_0\,\rho_0}\left[m\,k^2\,B_{z0}^2+k\,\frac{\mathrm{d}}{\mathrm{d}r}\,(B_{\theta0}\,B_{z0})+\frac{m^2-1}{r^2}\,\left(m\,B_{\theta0}^2-2\,r\,k\,B_{\theta0}\,B_{z0}\right)\right]\cos(m\theta-kz)\\ &+\hat{e}_\theta\,\frac{a}{\mu_0\,\rho_0}\left[k^2\,B_{z0}^2+\frac{m}{r}\,k\,B_{\theta0}\,B_{z0}\right]\sin(m\theta-kz)\\ &-\hat{e}_z\,\frac{a}{\mu_0\,\rho_0}\left[k^2\,B_{\theta0}\,B_{z0}+\frac{m}{r}\,k\,B_{\theta0}^2\right]\sin(m\theta-kz).\end{aligned}\tag{19}$$

Therefore the short time evolution of the helical perturbation (10) can now be approximately expressed by the time expansion

$$\boldsymbol{V}\,(\boldsymbol{X},t)\simeq\boldsymbol{V}_0(\boldsymbol{X})+\left(\frac{\mathrm{d}^2\boldsymbol{V}}{\mathrm{d}t^2}\right)_0\frac{t^2}{2!}.\tag{20}$$

A term proportional to (m^2-1) is a modification to the $m=1$ mode and if $m=1$, the results derived by Psimopoulos and Li are revealed.

4. Stability against ideal helical perturbations

It is obvious that the dynamics of each fluid element is transparent when the perturbation is explicitly expanded in time series (20) as in the above section. That is, a perturbation is unstable if the second order acceleration has the same direction as, and thus enhances, the initial perturbation. On the other hand, if a perturbation is unstable it must be strengthened and accordingly the second order acceleration should have the same direction as the initial perturbation. Therefore, it is not only a sufficient but also a necessary condition of instability that the initial perturbation and the second order acceleration have the same direction.

The stability of an ideal helical perturbation in a cylindrical Tokamak is explored below. By introducing the safety factor $q(r)=r\,B_z/R\,B_\theta$ and $k=n/R$, the second order acceleration $(\mathrm{d}^2\,\boldsymbol{V}/\mathrm{d}\,t^2)_0$ is converted to

$$\begin{aligned}\left(\frac{\mathrm{d}^2\boldsymbol{V}}{\mathrm{d}t^2}\right)_0 =&-\hat{e}_r\,\frac{a\,B_z^2}{\mu_0\,\rho\,R^2}\left[m\,n^2+n\,\frac{\mathrm{d}}{\mathrm{d}r}\,\left(\frac{r}{q}\right)+m\,\frac{m^2-1}{q^2}-2\,n\,\frac{m^2-1}{q}\right]\cos(m\theta-kz)\\ &+\hat{e}_\theta\,\frac{a\,m\,n\,B_z^2}{\mu_0\,\rho\,R^2}\,\left(\frac{n}{m}+\frac{1}{q}\right)\sin(m\theta-kz)\\ &-\hat{e}_z\,\frac{a\,m\,n\,B_\theta\,B_z}{\mu_0\,\rho\,R^2}\,\left(\frac{n}{m}+\frac{1}{q}\right)\sin(m\theta-kz),\end{aligned}\tag{21}$$

where for simplicity the subscript zero denoting equilibrium is omitted. The large aspect ratio assumption, $\epsilon=r/R<<1$, and $B_z\,R=R_0\,B_{z0}\left(1+O\left(\epsilon^2\right)\right)$ is obviously valid for a cylindrical Tokamak. Thus, the short

time evolution equation (20) can be expressed as follows:

$$\begin{aligned}\boldsymbol{V}(\boldsymbol{x},t) =&\hat{e}_r\, a\, m\, \cos(m\theta - kz)\left\{1 - \frac{B_z^2\, t^2}{2\,\mu_0\,\rho\, R^2}\left[n^2 + \frac{n}{m}\frac{\mathrm{d}}{\mathrm{d}r}\left(\frac{r}{q}\right) + \frac{m^2-1}{q^2} - 2\,n\frac{m^2-1}{m\,q}\right]\right\}\\ &- \hat{e}_\theta\, a\, \sin(m\theta - kz)\left[1 - \frac{m\,n\,B_z^2\,t^2}{2\,\mu_0\,\rho\,R^2}\left(\frac{n}{m} + \frac{1}{q}\right)\right]\\ &- \hat{e}_z\,\frac{a\,m\,n\,B_\theta\,B_z\,t^2}{2\,\mu_0\,\rho\,R^2}\left(\frac{n}{m} + \frac{1}{q}\right)\sin(m\theta - kz). \end{aligned} \tag{22}$$

It is found that the instability can be only produced by the r-direction perturbations because for a toroidal system, perturbations in the longitudinal direction is less dangerous and $(\mathrm{d}^2\boldsymbol{V}/\mathrm{d}t^2)_{0\theta}$ has different sign from $\boldsymbol{V}_{0\theta}$. The stability criterion c is hence obtained as

$$c \equiv -\left[n^2 + \frac{n}{m}\frac{\mathrm{d}}{\mathrm{d}\,r}\left(\frac{r}{q}\right) + \frac{m^2-1}{q^2} - 2\,n\,\frac{m^2-1}{m\,q}\right] \quad \begin{cases} > 0, & \text{unstable,} \\ < 0, & \text{stable.} \end{cases} \tag{23}$$

The criterion c comes from the r-component of (22). The term $-n\,\mathrm{d}\,(r/q)/\mathrm{d}\,r$ in Eq.(23) is related to the magnetic shear $s(r) \equiv r\,q'/q$:

$$-n\,\frac{\mathrm{d}}{\mathrm{d}r}\left(\frac{r}{q}\right) = \frac{n}{q}\,(s(r) - 1) \quad \begin{cases} > 0 & \text{instability enhanced,} \\ < 0 & \text{stability enhanced;} \end{cases} \tag{24}$$

so that in the positive shear region a strong shear will enhance instability or reduce stability while in the negative shear region the strong shear enhances stability or reduces instability.

In what follows, the stability of the ideal MHD helical perturbations is analysed according to criterion (23) by considering a type of example. Such analysis is based on the assumption that the total longitudinal current is constant or/and the poloidal magnetic flux is constant, namely

$$\begin{aligned} I_z &\equiv \int_0^{r_0} J_z\, r\, \mathrm{d}\, r\, \mathrm{d}\,\theta \\ &= \left.\frac{2\,\pi\, r^2\, B_z}{\mu_0\, R_0\, q}\right|_{r=r_0} = \text{Constant,} \end{aligned}$$

or/and

$$\Psi_p \sim \int_0^{r_0} B_\theta\, \mathrm{d}\, r = \int_0^{r_0} \frac{B_z\, r}{R\, q}\,\mathrm{d}\, r = \text{Constant,}$$

where $r_0 = 1$ is the normalized plasma boundary. The safety factor, $q(r)$, is taken as a function of the normalized minor radius:

$$q(r) \equiv \frac{q_0\,\alpha\,\left(1 + h\, r^{2\,p}\right)^{1+\frac{1}{p}}}{\alpha + h\, r^{2\,p}}, \tag{25}$$

where q_0 is the safety factor at zero, h, $0 < \alpha \leq 1$, $p = 1, 2, 3, 4\ldots$ are the positive parameters. The corresponding current density can be expressed as follows:

$$J_z(r) = \frac{2\,\alpha - 2\,h\,\left[-1 + p\,(-1+\alpha)\right] r^{2\,p}}{\alpha\, q_0\,\left(1 + h\, r^{2\,p}\right)^{2+\frac{1}{p}}}.$$

And the magnetic shear s satisfies

$$s = \frac{2\,p\,h\,r^{2\,p}}{1 + h\,r^{2\,p}}\left(\frac{1}{p} + \frac{\alpha - 1}{\alpha + h\,r^{2\,p}}\right) < 2.$$

Therefore, when $0 < \alpha < p/(1+p)$ the safety factor exists in negative shear region and corresponds to the RMS configuration.

Now the $m/n = 1/1$ mode will be studied in Sections 4.1 and 4.2 for PMS and RMS configurations, respectively, and the $m/n = 2/1$ mode in Section 4.3.

4.1. Local helical perturbations with $m/n = 1/1$: PMS configuration

First of all, the effect of different magnetic shear in the core region on the instability of $m/n = 1/1$ perturbation is considered for a monotonic q profile. For example, in Fig.1, the current density profiles, q profiles and stability criterion are shown as functions of normalized minor radius for different q_0. The solid, dashed and dash-dotted line respectively corresponds to the case with safety factor q_0=0.1, 0.2, and 0.3. The total current does not vary in these cases because q_1 is fixed at 2.4. A large q_0 corresponds to a week magnetic shear in the core region and a flattened current density profile. It is shown that the instability can be suppressed when q_0 increases. The perturbation

is unstable when $q_0 = 0.1$ whereas it becomes weakly unstable when $q_0 = 0.2$ and stable when $q_0 = 0.3$. Obviously, a larger q_0, which is here actually the $q_{\min}$, exhibits a weaker magnetic shear in the core and is favourable to the stability. This conclusion is similar to the previous results for internal kink mode predicted by Shafranov,[1] and Wesson.[2]

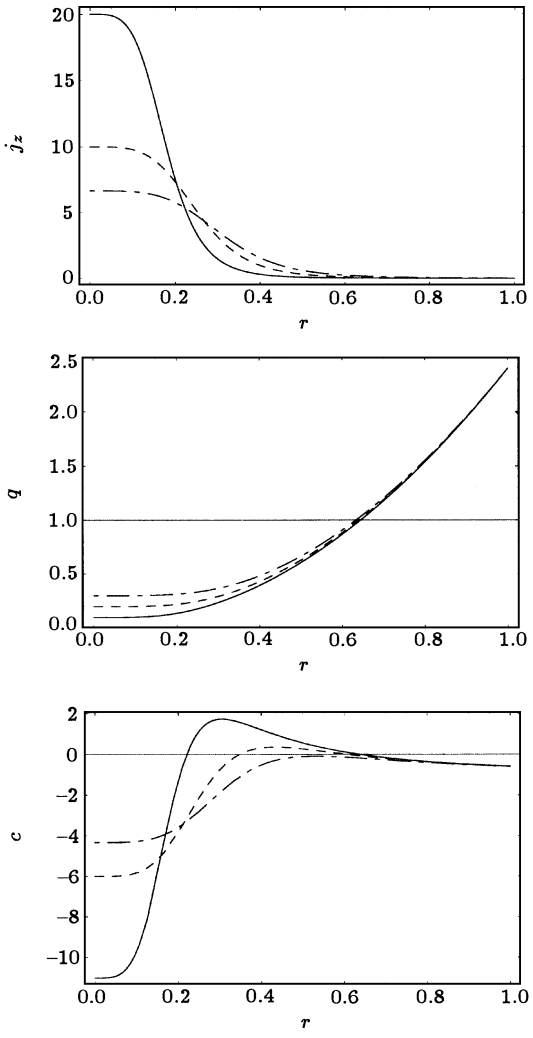


Fig.1. Current density, q profiles, and stability criterion for $m/n = 1/1$ perturbation in PMS configurations with $p = 2$, $q_1 = 2.4$: (a) solid line for $q_0 = 0.1$; (b) dashed line for $q_0 = 0.2$; (c) dash-dotted line for $q_0 = 0.3$.

Then, the effect of different magnetic shears in the intermediary region between the plasma core and the boundary is analysed on the instability of $m/n = 1/1$ perturbation for a monotonic q profile. For example, the current density profiles, q profiles and stability criterion are shown as functions of normalized minor radius with different p in Fig.2. The solid, dashed and dash-dotted line corresponds to the case with p=1, 2, and 4, respectively, and they all have the same q_0 (which is also $q_{\min}$) which assures that the instability is not altered by the minimum safety factor $q_{\min}$ but by other factors only. The total current still does not vary in the three cases due to the fixed q_1 (2.4). It is found that when p increases the magnetic shear becomes stronger and current density becomes steeper in the middle region so that strong instability can be triggered. The perturbation is stable when $p = 1$ whereas it becomes unstable when $p = 2$ and more unstable when $p = 4$. Thus, larger p produces a stronger magnetic shear in the middle region and is unfavourable to the stability.

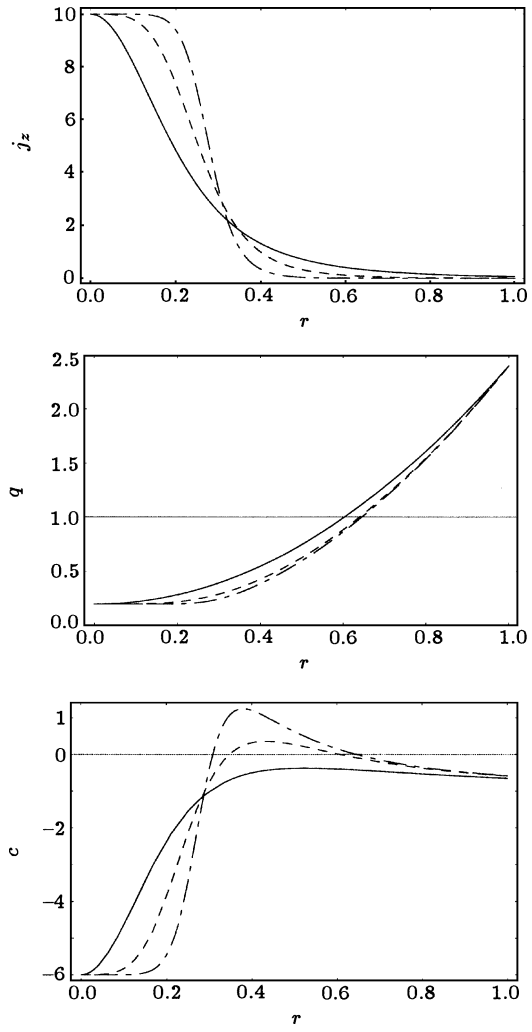


Fig.2. Current density, q profiles, and stability criterion for $m/n = 1/1$ perturbation in PMS configurations with $q_0 = 0.2$, $q_1 = 2.4$: (a) solid line for $p = 1$; (b) dashed line for $p = 2$; (c) dash-dotted line for $p = 4$.

4.2. Local helical perturbations with $m/n = 1/1$: RMS configuration

In this section, the question of whether local helical perturbations for the RMS mode are more stable than that of the PMS configuration is investigated.

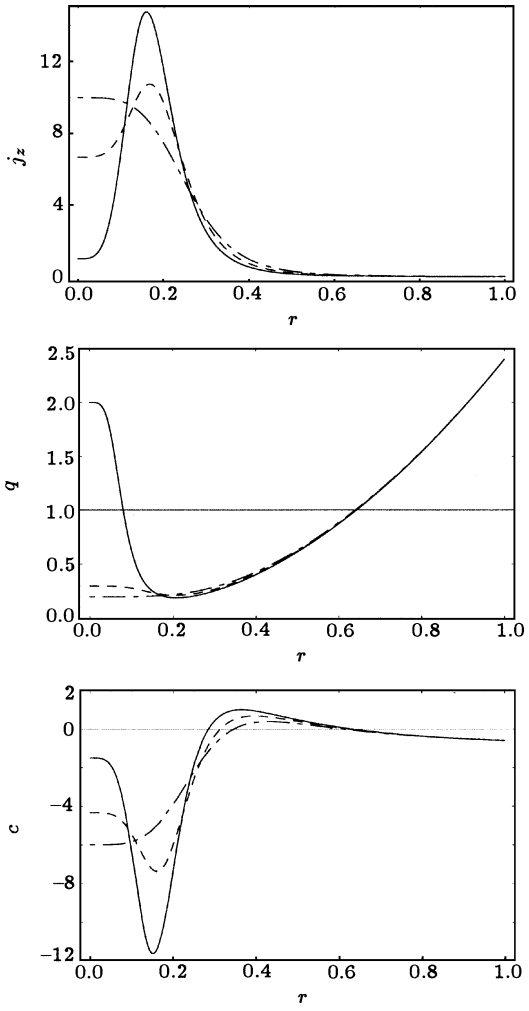


Fig.3. Current density, q profiles, and stability criterion for $m/n = 1/1$ perturbation in PMS and RMS configurations with $p = 2$, $q_1 = 2.4$: (a) solid line for $q_0 = 2$ (RMS mode); (b) dashed line for $q_0 = 0.3$ (RMS mode); (c) dash-dotted line for $q_0 = 0.2$ (PMS mode).

First, the effect of reversed magnetic shear in the plasma core on the instability of $m/n = 1/1$ perturbation is considered for a non-monotonic q profile corresponding to a RMS configuration. For example, the current density profiles, q profiles and stability criterion are shown as functions of normalized minor radius with different q_0 in Fig.3. The dash-dotted line corresponds to the case with $q_0 = 0.1$ in a PMS configuration. The dashed and solid line respectively corresponds to the case with $q_0 = 2$ and 0.3 in RMS configurations. The poloidal magnetic flux is fixed; besides, the total current does not alter in the three cases. As in the previous section, to separate the other effects from that of different $q_{\min}$ the three lines have the same $q_{\min}$. It is shown that instability is enhanced when q_0 increases; meanwhile the positive magnetic shear increases and the centre magnetic shear changes from positive to negative. The mode is weakly unstable when $q_0 = 0.1$ and becomes more unstable when $q_0 = 0.3$ and $q_0 = 2$. Obviously, larger q_0 corresponds to stronger negative magnetic shear in the core and stronger positive magnetic shear in the middle for the RMS configuration, which is unfavourable to the stability. These results indicate that the stability of RMS configuration is not better than that of the PMS configuration.

Next, we discuss how the shift of minimum $q_{\rm m}$ in the RMS configuration influences the instability of $m/n = 1/1$ perturbation with a non-monotonic q profile. For example, the current density profiles, q profiles and stability criterion are shown as functions of normalized minor radius for different p in Fig.4. The

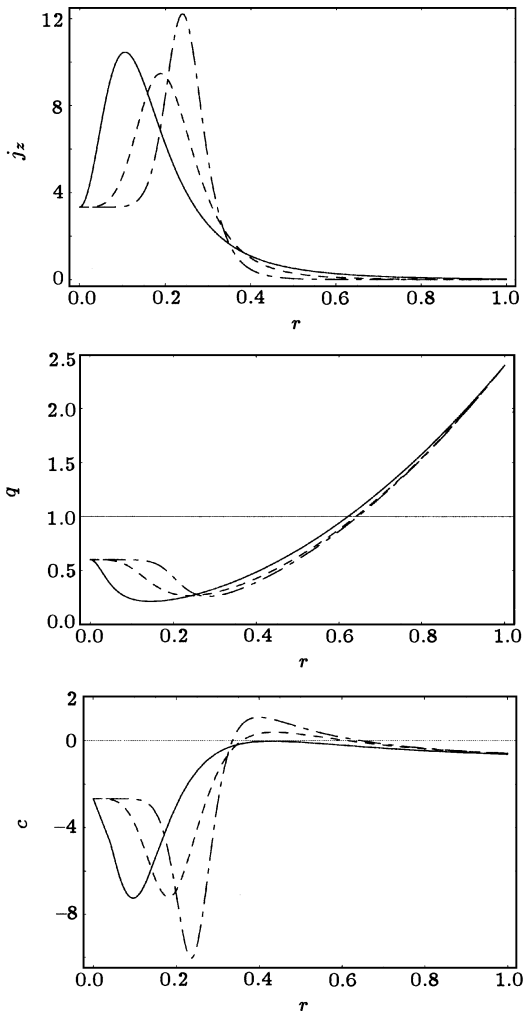


Fig.4. Current density, q profiles, and stability criterion for $m/n = 1/1$ perturbation in RMS configurations with $q_0 = 0.6$, $q_1 = 2.4$: (a) solid line for $p = 1$; (b) dashed line for $p = 2$; (c) dash-dotted line for $p = 4$.

solid, dash and dash-dotted line respectively correspond to the case with p=1, 2 and 4 and a non-monotonic q for $q_0 = 0.6$, $q_1 = 2.4$. The poloidal magnetic flux and the total current remain unchanged in the three cases. Although the solid line has a smaller minimum safety factor $q_{\min}$, its positive magnetic shear is weaker than those of the other two. The dash and dash-dotted line have the same $q_{\min}$ but the dash-dotted line has a stronger positive magnetic shear than the dash line. It is found that the instability can be enhanced as p increases and the minimum $q_{\rm m}$ is shifted form the core toward the middle region because the positive magnetic shear increases accordingly. The perturbation with $m/n = 1/1$ is marginal stable as $p = 1$ whereas it becomes unstable as $p = 2$ and more unstable as $p = 4$. Similar to the monotonic q profile case, larger p corresponding to stronger magnetic shear in the middle is unfavourable to the stability.

4.3. Local helical perturbations with $m/n = 2/1$

We can adopt a similar approach to study the instability of perturbations with $m/n = 2/1$. It is hard to find instability for $m \geq 2$ mode because the stabilizing terms in Eq.(23) are enhanced as m increases. For simplicity, we only discuss two examples in Figs.5 and 6 where the stability of $m/n = 2/1$ perturbation are shown respectively in the case of the PMS mode and RMS mode. No instability is found in both cases even though the current density and q profiles are respectively similar to the cases in Figs.1 and 3. Our conclusions is that the instabilities of $m/n = 2/1$ perturbations act very differently from those of $m/n = 2/1$ and therefore non-local perturbations with $m \geq 2$ should be considered, which is confirmed by a previous work.[15]

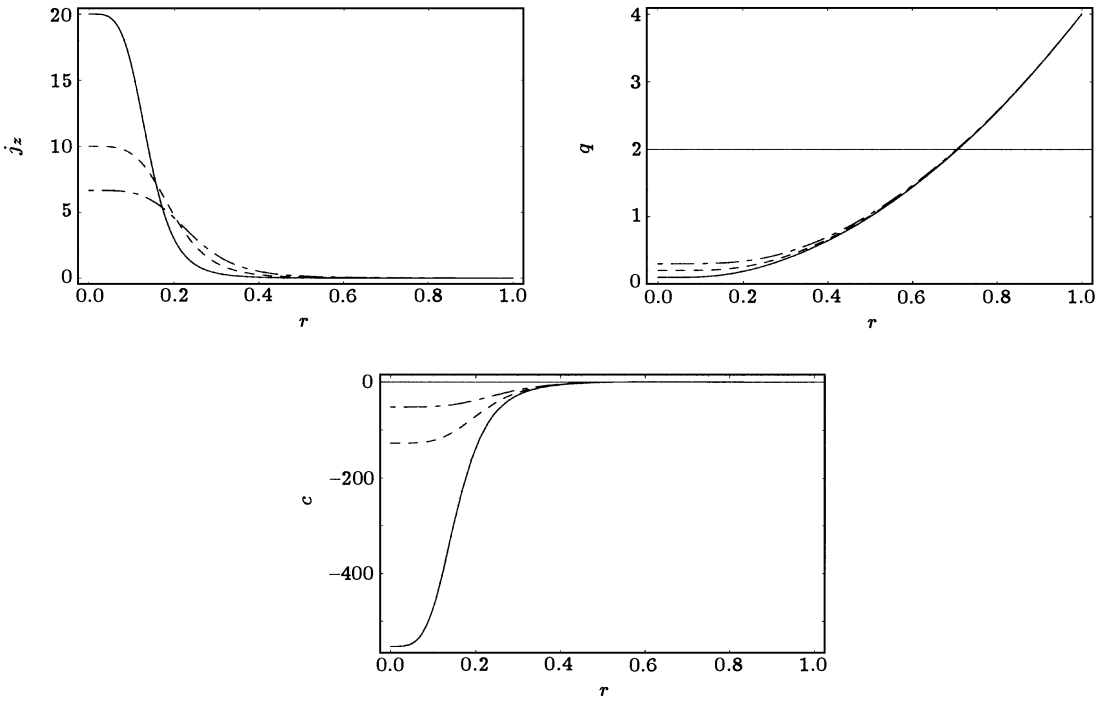


Fig.5. Current density, q profiles, and stability criterion for $m/n = 2/1$ perturbation in PMS configurations with $p = 2$, $q_1 = 4$: (a) solid line for $q_0 = 0.1$; (b) dashed line for $q_0 = 0.2$; (c) dash-dotted line for $q_0 = 0.3$.

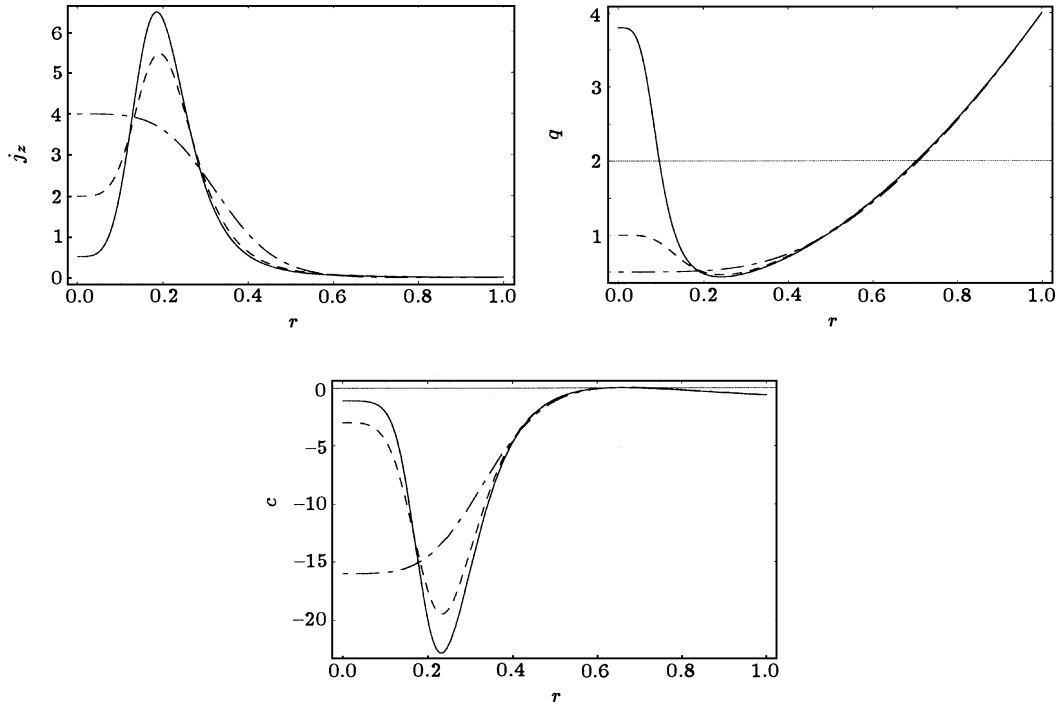


Fig.6. Current density, q profiles, and stability criterion for $m/n = 2/1$ perturbation in PMS and RMS configurations with $p = 2$, $q_1 = 4$: (a) solid line for $q_0 = 3.8$ (RMS mode); (b) dashed line for $q_0 = 1$ (RMS mode); (c) dash-dotted line for $q_0 = 0.5$ (PMS mode).

5. Conclusion

In this paper we have investigated the evolution and the stability properties of local helical perturbations with $m \geq 1$ in a cylindrical plasma for an arbitrary magnetic shear configuration. An analytic criterion has been obtained and the stability properties of cylindrical Tokamak have been studied by considering a specific $q(r)$ profile.

The time expanding method describes the early time evolution of perturbations in plasma. An expression (19) that describes the evolution of a helical perturbation (10) in cylindrical plasma has been obtained by employing the ideal MHD equations. This result is transformed to (22) for a cylindrical Tokamak under the large aspect ratio assumption. Then, the general criteria (23) are obtained directly by comparing the second order acceleration with the initial perturbation. These criteria predict that:

1. In the positive shear region a strong shear will enhance instability while in the negative shear region the strong shear enhances stability.

2. The $m = 1$ mode is the most unstable mode because the stabilizing terms in the criterion (23) are enhanced as m increases.

These analytical conclusions have been well confirmed by the study on the stability properties of local helical perturbations in cylindrical Tokamaks, where a specific $q(r)$ profile is taken as function (25). Under the conditions that the total current is constant or/and the poloidal magnetic flux is constant, the following results have been obtained:

1. For perturbations with $m/n = 1/1$ in a PMS configuration, a larger q_0, i.e. $q_{\min}$, exhibits a weaker magnetic shear in the core and is favourable to the stability. A larger p produces a stronger shear in the middle region and is unfavourable to the stability.

2. For perturbations with $m/n = 1/1$ in an RMS configuration, a larger q_0 corresponds to a stronger negative magnetic shear in the core and stronger positive magnetic shear in the middle, which is unfavourable to the stability. A larger p corresponding to stronger magnetic shear in the middle is unfavourable to the stability.

3. No instabilities are found for local perturbations with $m/n = 2/1$. Thus, the instabilities of $m/n = 2/1$ perturbations act very differently from those of $m/n = 2/1$ and non-local perturbations with $m \geq 2$ should be considered, which is confirmed by the work of Ref.[15].

4. The stability for the RMS configuration is not better than that for the PMS configuration.

Although a reasonable stability picture has been obtained for cylindrical Tokamak, what has been

adopted in this paper is not a real toroidal system. The geometric effects of toroidicity shall give some modification to the present results. The assumption of ideal MHD imposes the constraint of fixed topology on the magnetic field structure which causes an overestimate of the stability. The method is readily extended to the stabilities in a toroidal regime. This will be the subject of a future work.

References

[1] Shafranov V D 1970 *Sov. Phys. Tech. Phys.* **15** 175

[2] Wesson J A 1978 *Nucl. Fusion* **18** 87

[3] Bateman G 1978 *MHD Instabilities* (Cambridge, MA: MIT Press)

[4] Freidberg J P 1982 *Rev. Mod. Phys.* **53** 801

[5] Mirnov S, Wesley J, Fujisawa N and Gribov Y 1999 *Nucl. Fusion* **39** 2251

[6] Kessel C, Manickam J, Rewoldt G and Tang W M 1994 *Phys. Rev. Lett.* **72** 1212

[7] Levinton F M, Zarnstorff M C, Batha S H, Bell M, Bell R E, Budny R V, Bush C, Chang Z, Fredrickson E, Janos A, Manickam J, Ramsey A, Sabbagh S A, Schmidt G L, Synakowski E J and Taylor G 1995 *Phys. Rev. Lett.* **75** 4417

[8] Strait E J, Lao L L, Mauel M E, Rice B W, Taylor T S, Burrell K H, Chu M S, Lazarus E A, Osborne T H, Thompson S J and Turnbull A D 1995 *Phys. Rev. Lett.* **75** 4421

[9] Lazarus E A *et al* 1996 *Phys. Rev. Lett.* **77** 2714

[10] Gimblett C G, Hastie R J and Hender T C 1996 *Phys. Plasmas* **3** 3369

[11] Gunter S, Schade S, Maraschek M, Pinches S D, Strumberger E, Wolf R and Yu Q 2000 *Nucl. Fusion* **40** 1541

[12] Takeji S, Tokuda S, Fujita T, Suzuki T, Isayama A, Ide S, Ishii Y, Kamada Y, Koide Y, Matsumoto T, Oikawa T, Ozeki T and Sakamoto Y 2002 *Nucl. Fusion* **42** 5

[13] Psimopoulos M and Haines M G 1986 *Plasma Phys. and Control. Fusion* **28** 917

[14] Psimopoulos M and Li D 1993 *Plasma Phys. Control. Fusion* **35** 467

[15] Zhang W and Li D 2004 *Phys. Plasmas* **11** 1987